

Locating periodic orbits by Topological Degree theory

C.Polymilis^a, G. Servizi^b, Ch. Skokos^{c,d}, G. Turchetti^b & M. N. Vrahatis^e ¹

^a*Department of Physics, University of Athens, Panepistimiopolis, GR-15784 Zografos, Athens, Greece*

^b*Department of Physics, Bologna University, Via Irnerio 46, I-40126 Bologna, Italy and I.N.F.N. Sezione di Bologna, Via Irnerio 46, I-40126 Bologna, Italy*

^c*Department of Mathematics, Division of Applied Analysis and Center for Research and Applications of Nonlinear Systems (CRANS), University of Patras, GR-26500 Patras, Greece*

^d*Research Center for Astronomy, Academy of Athens, 14 Anagnostopoulou str., GR-10673 Athens, Greece*

^e*Department of Mathematics and University of Patras Artificial Intelligence Research Center (UPAIRC), University of Patras, GR-26110 Patras, Greece*

Abstract

We consider methods based on the topological degree theory to compute periodic orbits of area preserving maps. Numerical approximations of the Kronecker integral and the application of Stenger's method allows us to compute the value of the topological degree in a bounded region of the phase space. If the topological degree of an appropriate set of equations has a non-zero value, we know that there exists at least one periodic orbit of a given period in the given region. We discuss in detail the problems that these methods face, due to the existence of periodic orbits near the domain's boundary and due to the discontinuity curves that appear in maps defined on the torus. We use the characteristic bisection method for actually locating periodic orbits. We apply this method successfully, both to the standard map, which is a map defined on the torus, and to the beam-beam map which is a continuous map on the plane. Specifically we find a large number of periodic orbits of periods up to 40, which give us a clear picture of the dynamics of both maps.

1 The topological degree (TD) and its computation

We consider the problem of finding the solutions of a system of nonlinear equations of the form

$$F_n(x) = \Theta_n, \quad (1)$$

where $F_n = (f_1, f_2, \dots, f_n) : D_n \subset \mathbb{R}^n \rightarrow \mathbb{R}^n$ is a function from a domain D_n into \mathbb{R}^n , $\Theta_n = (0, 0, \dots, 0)$ and $x = (x_1, x_2, \dots, x_n)$. The above system can be written as:

$$\begin{aligned} f_1(x_1, x_2, \dots, x_n) &= 0, \\ f_2(x_1, x_2, \dots, x_n) &= 0, \\ &\vdots \\ f_3(x_1, x_2, \dots, x_n) &= 0. \end{aligned} \quad (2)$$

The topological degree (TD) theory gives us information on the existence of solutions of the above system, their number and their nature [5, 9, 10, 3, 6]. Kronecker introduced the concept of the TD in 1869 [5], while Picard in 1892 [9] succeeded in providing a theorem for computing the exact number of solutions of system (1). Numerical methods based on the TD theory have been applied successfully to numerous dynamical systems (e.g. [16, 17, 18, 19, 4, 8]).

¹E-mails: servizi@bo.infn.it (G. S.), hskokos@cc.uoa.gr (Ch. S.), turchett@bo.infn.it (G. T.), vrahatis@math.upatras.gr (M. N. V.)

In order to define the concept of the topological degree we consider the function F_n of system (1) to be continuous on the closure $\overline{D_n}$ of D_n , satisfying also $F_n(x) \neq \Theta_n$ for x on the boundary $b(D_n)$ of D_n . We also consider the solutions of (1) to be simple i.e. the determinant of the corresponding Jacobian matrix (J_{F_n}) at the solution, to be different from zero. Then the *topological degree (TD) of F_n at Θ_n relative to D_n* is defined as:

$$\deg[F_n, D_n, \Theta_n] = \sum_{x \in F_n^{-1}(\Theta_n)} \text{sgn}(\det J_{F_n}(x)) = N_+ - N_-, \quad (3)$$

where $\det J_{F_n}$ is the determinant of the Jacobian matrix of F_n , sgn is the well-known sign function, N_+ the number of roots with $\det J_{F_n} > 0$ and N_- the number of roots with $\det J_{F_n} < 0$. It is evident that if a nonzero value of $\deg[F_n, D_n, \Theta_n]$ is obtained then there exist at least one solution of system $F_n(x) = \Theta_n$ within D_n [5].

A practical way to find the TD is the computation of Kronecker integral [5]. In particular, under the assumptions of the above-mentioned definition of the TD the $\deg[F_n, D_n, \Theta_n]$ can be computed as:

$$\deg[F_n, D_n, \Theta_n] = \frac{\Gamma(n/2)}{2\pi^{n/2}} \int \int_{b(D_n)} \dots \int \frac{\sum_{i=1}^n A_i dx_i \dots dx_{i-1} dx_{i+1} \dots dx_n}{(f_1^2 + f_2^2 + \dots + f_n^2)^{n/2}} \quad (4)$$

where

$$A_i = (-1)^{n(i-1)} \begin{vmatrix} f_1 & \frac{\partial f_1}{\partial x_1} & \dots & \frac{\partial f_1}{\partial x_{i-1}} & \frac{\partial f_1}{\partial x_{i+1}} & \dots & \frac{\partial f_1}{\partial x_n} \\ f_2 & \frac{\partial f_2}{\partial x_1} & \dots & \frac{\partial f_2}{\partial x_{i-1}} & \frac{\partial f_2}{\partial x_{i+1}} & \dots & \frac{\partial f_2}{\partial x_n} \\ \vdots & \vdots & & \vdots & \vdots & & \vdots \\ f_n & \frac{\partial f_n}{\partial x_1} & \dots & \frac{\partial f_n}{\partial x_{i-1}} & \frac{\partial f_n}{\partial x_{i+1}} & \dots & \frac{\partial f_n}{\partial x_n} \end{vmatrix}, \quad (5)$$

and $\Gamma(x)$ is the gamma function.

In order to find the number N of solutions of system (1) we consider the function

$$F_{n+1} = (f_1, f_2, \dots, f_n, f_{n+1}) : D_{n+1} \subset \mathbb{R}^{n+1} \rightarrow \mathbb{R}^{n+1}, \quad (6)$$

where

$$f_{n+1} = y \det J_{F_n}, \quad (7)$$

$\mathbb{R}^{n+1} : x_1, x_2, \dots, x_n, y$ and D_{n+1} is the product of D_n with a real interval on the y -axis containing $y = 0$. Then the exact number N of the solutions of equation $F_n(x) = \Theta_n$ is proven to be [9]:

$$N = \deg[F_{n+1}, D_{n+1}, \Theta_{n+1}]. \quad (8)$$

By applying this result and using the computation of TD by Kronecker integral (4) in the case of a set of two equations:

$$\begin{aligned} f_1(x_1, x_2) &= 0, \\ f_2(x_1, x_2) &= 0, \end{aligned} \quad (9)$$

we find that the number N of roots in the domain $D_2 = [a, b] \times [c, d]$ is given by:

$$N = \frac{1}{2\pi} \int_{b(D_2)} (P_1 dx_1 + P_2 dx_2) + \epsilon \int \int_{D_2} \frac{Q dx_1 dx_2}{(f_1^2 + f_2^2 + \epsilon^2 J^2)^{3/2}}, \quad (10)$$

where ϵ is an arbitrary positive value, and

$$P_i = \frac{\left(f_1 \frac{\partial f_2}{\partial x_i} - f_2 \frac{\partial f_1}{\partial x_i} \right) \epsilon J}{(f_1^2 + f_2^2)(f_1^2 + f_2^2 + \epsilon^2 J^2)^{1/2}}, \quad i = 1, 2 \quad Q = \begin{vmatrix} f_1 & \frac{\partial f_1}{\partial x_1} & \frac{\partial f_1}{\partial x_2} \\ f_2 & \frac{\partial f_2}{\partial x_1} & \frac{\partial f_2}{\partial x_2} \\ J & \frac{\partial J}{\partial x_1} & \frac{\partial J}{\partial x_2} \end{vmatrix}, \quad (11)$$

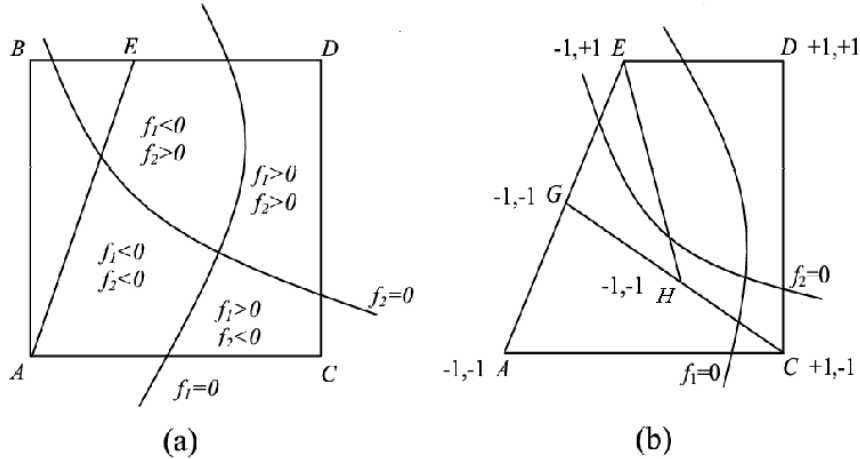


Figure 1: (a) The polyhedron ABDC is noncharacteristic while the polyhedron AEDC is characteristic. (b) Application of the characteristic bisection method to the characteristic polyhedron AEDC, giving rise to the polyhedra GEDC and HEDC, which are also characteristic.

with J denoting the determinant of the Jacobian matrix of $F_2 = (f_1, f_2)$.

Another method for computing the TD of F_n at a domain D_n is the application of Stenger's theorem [12, 7]. Following this approach for finding the TD, we only need to know the signs of functions f_1, f_2, \dots, f_n in a 'sufficient' set of points on the boundary $b(D_n)$ of D_n .

2 The characteristic bisection method

The characteristic bisection method is based on the characteristic polyhedron concept for the computation of roots of the equation (1). The construction of a suitable n -polyhedron, called the characteristic polyhedron, can be done as follows. Let M_n be the $2^n \times n$ matrix whose rows are formed by all possible combinations of -1 and 1 . Consider now an oriented n -polyhedron Π^n , with vertices $V_k, k = 1, \dots, 2^n$. If the $2^n \times n$ matrix of signs associated with F and Π^n , whose entries are the vectors

$$\text{sgn}F_n(V_k) = (\text{sgn}f_1(V_k), \text{sgn}f_2(V_k), \dots, \text{sgn}f_n(V_k)), \quad (12)$$

is identical to M_n , possibly after some permutations of these rows, then Π^n is called the characteristic polyhedron relative to F_n . If F_n is continuous, then, after some suitable assumptions on the boundary of Π^n we have:

$$\deg[F_n, \Pi^n, \Theta_n] = \pm 1 \neq 0. \quad (13)$$

This means that there is at least one solution of system $F_n(x) = \Theta_n$ within Π^n .

To clarify the characteristic polyhedron concept we consider a function $F_2 = (f_1, f_2)$. Each function $f_i, i = 1, 2$, separates the space into a number of different regions, according to its sign, for some regions $f_i < 0$ and for the rest $f_i > 0, i = 1, 2$. Thus, in figure 1(a) we distinguish between the regions where $f_1 < 0$ and $f_2 < 0, f_1 < 0$ and $f_2 > 0, f_1 > 0$ and $f_2 > 0, f_1 > 0$ and $f_2 < 0$. Clearly, the following combinations of signs are possible: $(-, -), (-, +), (+, +)$ and $(+, -)$. Picking a point, close to the solution, from each region we construct a characteristic polyhedron. In this figure we can perceive a characteristic and a noncharacteristic polyhedron Π^2 . For a polyhedron Π^2 to be characteristic all the above combinations of signs must appear at its vertices. Based on this criterion, polyhedron ABDC is not a characteristic polyhedron, whereas AEDC is. A characteristic polyhedron can be considered as a translation of Poincaré-Miranda hypercube [15].

Next, we describe the characteristic bisection method. This method simply amounts to constructing another refined characteristic polyhedron, by bisecting a known one, say Π^n , in order to determine the solution with the desired accuracy. We compute the midpoint M of an one-dimensional edge of Π^n , e.g. $\langle V_i, V_j \rangle$. The endpoints of this one-dimensional line segment are vertices of Π^n , for which the corresponding coordinates of the vectors, $\text{sgn}F_n(V_i)$ and $\text{sgn}F_n(V_j)$ differ from each other only in one entry. To obtain another characteristic polyhedron we compare the sign of $F_n(M)$ with that of $F_n(V_i)$ and $F_n(V_j)$ and substitute M for that vertex for which the signs are identical. Subsequently, we reapply the aforementioned technique to a different edge (for details we refer the reader to [13, 14, 16, 8]).

To fully comprehend the characteristic bisection method we illustrate in figure 1(b) its repetitive operation on a characteristic polyhedron Π^2 . Starting from the edge AE we find its midpoint G and then calculate its vector of signs, which is $(-1, -1)$. Thus, vertex G replaces A and the new refined polyhedron GEDC, is also characteristic. Applying the same procedure, we further refine the polyhedron by considering the midpoint H of GC and checking the vector of signs at this point. In this case, its vector of signs is $(-1, -1)$, so that vertex G can be replaced by vertex H. Consequently, the new refined polyhedron HEDC is also characteristic. This procedure continues up to the point that the midpoint of the longest diagonal of the refined polyhedron approximates the root within a predetermined accuracy.

3 Applications

We apply methods based on the topological degree theory to compute periodic orbits of two area preserving maps, the Standard map (SM) [2], which is a map defined on the torus:

$$\begin{aligned} x' &= x + y - \frac{k}{2\pi} \sin(2\pi x) \\ y' &= y - \frac{k}{2\pi} \sin(2\pi x) \end{aligned} \quad , \quad \text{mod}(1), \quad x, y \in [-0.5, 0.5], \quad (14)$$

and the beam-beam map (BM) [1, 11], which is a map defined on \mathbb{R}^2 :

$$\begin{aligned} x' &= x \cos(2\pi\omega) + (y + 1 - e^{-x^2}) \sin(2\pi\omega), \\ y' &= -x \sin(2\pi\omega) + (y + 1 - e^{-x^2}) \cos(2\pi\omega). \end{aligned} \quad (15)$$

Given a dynamical map $M : \{x' = g_1(x, y), y' = g_2(x, y)\}$, the periodic points of period p are fixed points of the p -iteration M^p of the map and the zeroes of the function:

$$F = M^p - I = \begin{cases} f_1 &= g_1^p(x, y) - x \\ f_2 &= g_2^p(x, y) - y \end{cases} \quad , \quad (16)$$

where I is the identity.

One can use a color map to inspect the geometry of function F (16) and to locate its zeroes. The color map is created by choosing a lattice of $m \times m$ points and by associating to each point a color chosen according to the signs of the functions f_1, f_2 as shown in figure 2. A simple algorithm allows to detect the cells, formed by the lattice of $m \times m$ points, whose vertices have different colors. A cell is a candidate to have a zero in its interior if the corresponding topological degree is found to be different from zero. In figures 3 and 4 we construct the color map and apply the above mentioned algorithm for locating periodic orbits of period 3 for the SM and of period 5 for the BM, respectively. In both figures the gray circles at the right panels denote the positions of the found periodic orbits. We see that for both maps some periodic orbits were not found because some of the four color domains close to the fixed point were very thin. On the other hand, due to the discontinuity of function F (16), some zeros that do not correspond to real periodic orbits were found for the SM (right panel of figure 3).

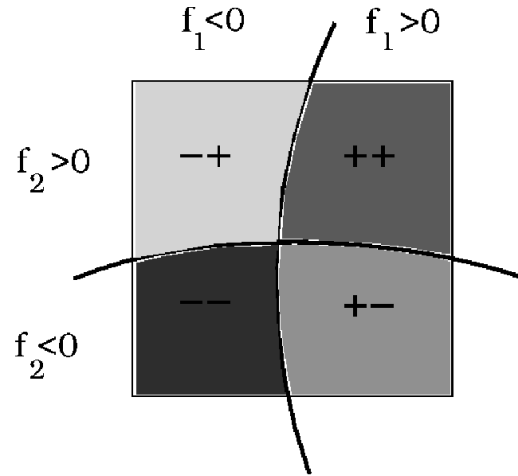


Figure 2: Sketch of the domains where functions f_1 and f_2 of system (16) have a definite sign.

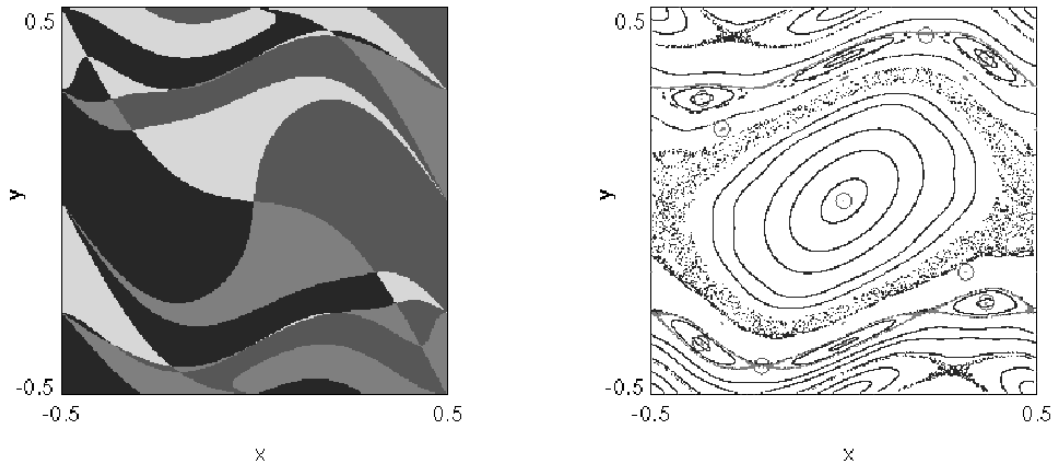


Figure 3: Standard map (14) for $k = 0.9$: color map for $p = 3$ iterations of the map computed on a square of $m \times m$ points for $m = 512$ (left panel); phase plot of the map (right panel). The gray circles denote the positions of the zeros of the corresponding function (16).

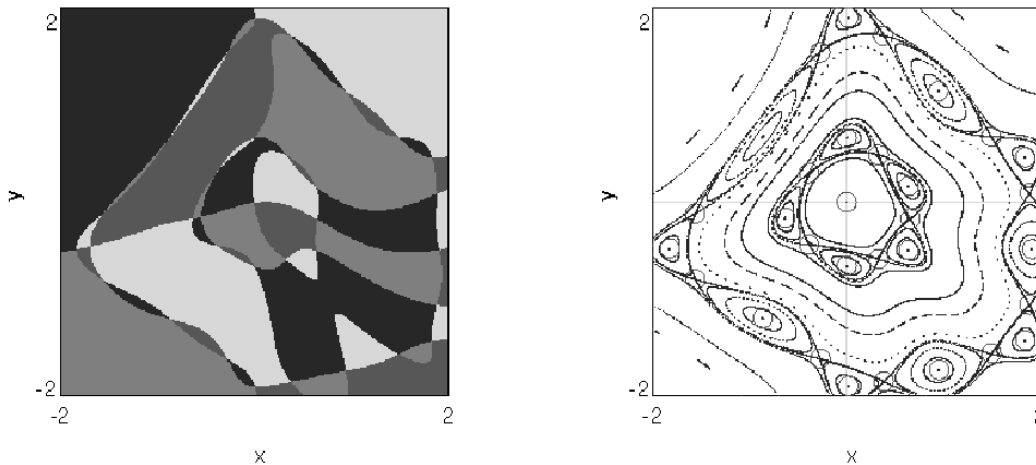


Figure 4: Beam-beam map (15) for $\omega = 0.21$: color map for $p = 5$ iterations of the map computed on a square of $m \times m$ points for $m = 512$ (left panel); phase plot of the map (right panel). The gray circles denote the positions of the zeros of the corresponding function (16).

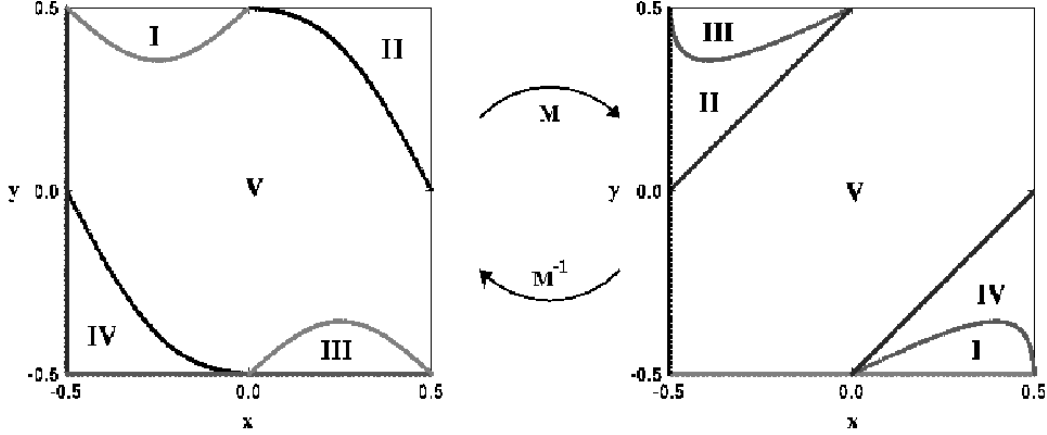


Figure 5: The discontinuity curves of the standard map M (14) divide the phase space in five continuous regions (I, II, III, IV, V). In each region the computation of the TD can be performed accurately.

For maps defined on the torus like the SM (14), the computation of the TD using Stenger's method or the Kronecker integral (10) faces problems due to the presence of discontinuity curves. Indeed Kronecker integral is defined on a domain where the function F (16) is continuous.

For the SM the discontinuity curves are the lines $x = -0.5$ and $y = -0.5$. By applying the SM map M once these lines are mapped on the curves seen in the right panel of figure 5. On the initial phase space there exist also the discontinuity curves that will be mapped after one iteration to the lines $x = -0.5$ and $y = -0.5$. These curves are also plotted in the left panel of figure 5. These curves can be produced by applying the inverse SM to the discontinuity lines $x = -0.5$ and $y = -0.5$. So the discontinuity curves divide the initial phase space in five continuous regions marked as I, II, III, IV and V in figure 5. In each region the computation of the TD can be performed accurately by Stenger's method or by evaluating Kronecker integral. If, however, the boundary of the domain where these procedures are applied, cross a discontinuity curve the results we get are not correct (figure 6).

In order to study the dependence of the procedure for finding the TD in a region D , with respect to the distance of a root from the boundary of D , we consider the simple map

$$F^* = (f_1, f_2) = \begin{cases} f_1(x, y) = y - \frac{x^3}{3} + x \\ f_2(x, y) = y \end{cases} . \quad (17)$$

The lines $f_1 = 0$, $f_2 = 0$ are plotted in figure 7(a). The system $F^* = (0, 0)$ has three roots. The determinant of the corresponding Jacobian matrix ($\det J_{F^*}$) is positive for root $(0, 0)$ and negative for roots $(-\sqrt{3}, 0)$ and $(\sqrt{3}, 0)$. We also consider a rectangular of the form $[-a, 2] \times [-2, 2]$ with $a > \sqrt{3}$, shown in figure 7(a). Since this domain contains the three roots of the system the value of the TD is -1 . We set $a = \sqrt{3} + \epsilon$ with $\epsilon > 0$ so that the boundary approaches the root as $\epsilon \rightarrow 0$, as shown by the arrow in figure 7(a). We compute the TD for different values of ϵ applying Stenger's method, by using the same number of points m on every side of the rectangle. We denote by $n_{gp} = 4m$ the smallest number of grid points needed to compute the TD with certainty. In figure 7(b) we plot in log-log scale, n_{gp} with respect to ϵ (dashed line). The slope of the curve is almost -1 so that $m \propto \epsilon^{-1}$. The same result holds for any map when the boundary approaches a root (the solid line in figure 7(b) is obtained for a similar example for the SM (14)).

Despite the problems caused by the discontinuity curves or by roots located very close to the domain's boundary, the use of the characteristic bisection method

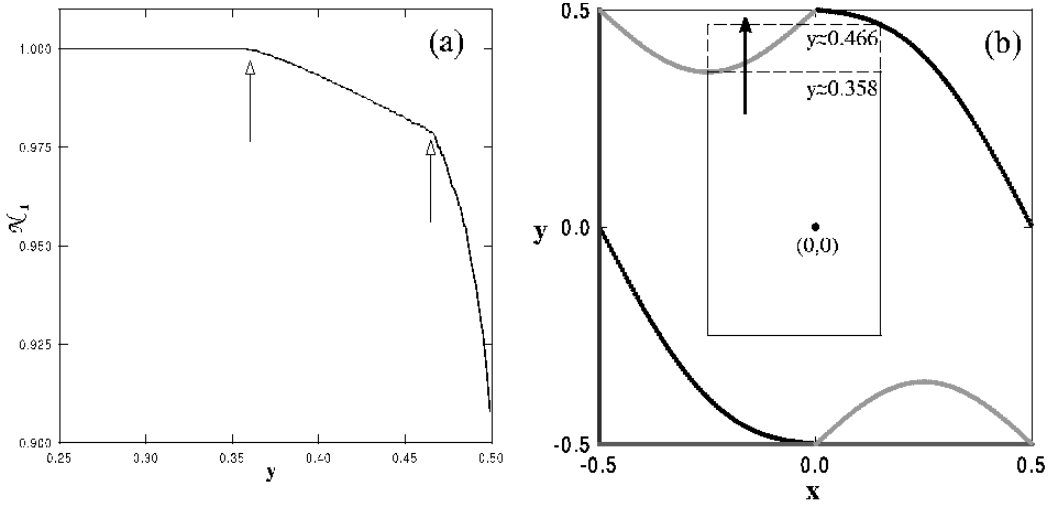


Figure 6: (a) Number of period 1 fixed points \mathcal{N}_1 evaluated for the SM (14) with $k = 0.9$ using the Kronecker integral (10), in a rectangular domain whose upper-side moves, as a function of the y coordinate of this side. The rectangle and the discontinuity lines are shown in (b). For the various rectangles, \mathcal{N}_1 should be equal to 1 since they contain only 1 fixed point of period 1, namely point $(0,0)$. The two points marked by arrows in (a) where \mathcal{N}_1 deviates from the correct value $\mathcal{N}_1 = 1$, correspond to $y \approx 0.358$ and $y \approx 0.466$ respectively, where the upper-side of the rectangular crosses the two discontinuity curves in (b).

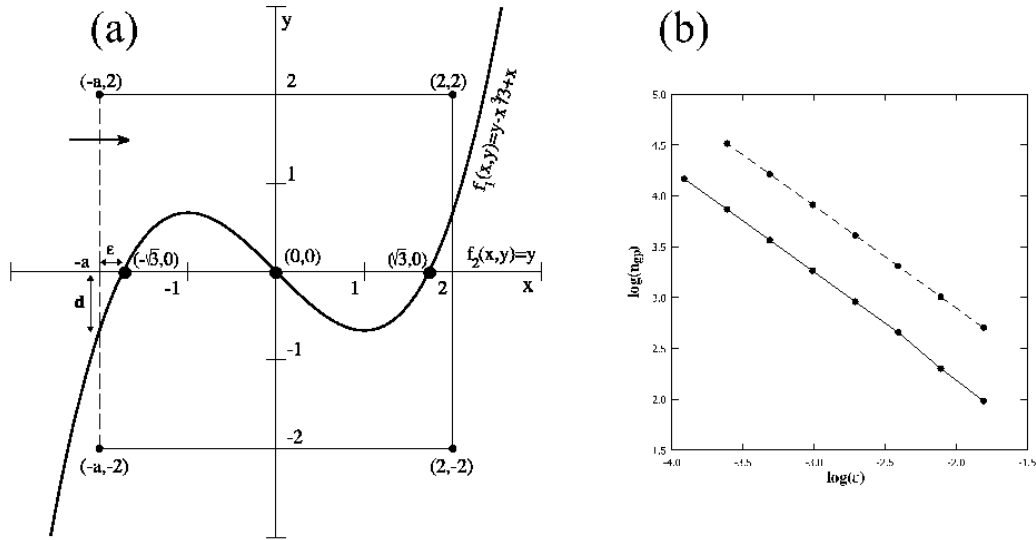


Figure 7: (a) Plot of the curves $f_1 = y - \frac{x^3}{3} + x = 0$, $f_2 = y = 0$ (b) Dependence of the number of grid points n_{gp} , needed for computing the correct value of the TD in a domain, on the distance ϵ of a root from the boundary of the domain, for the set of equations of (a) (dashed line) and the SM (continuous line).

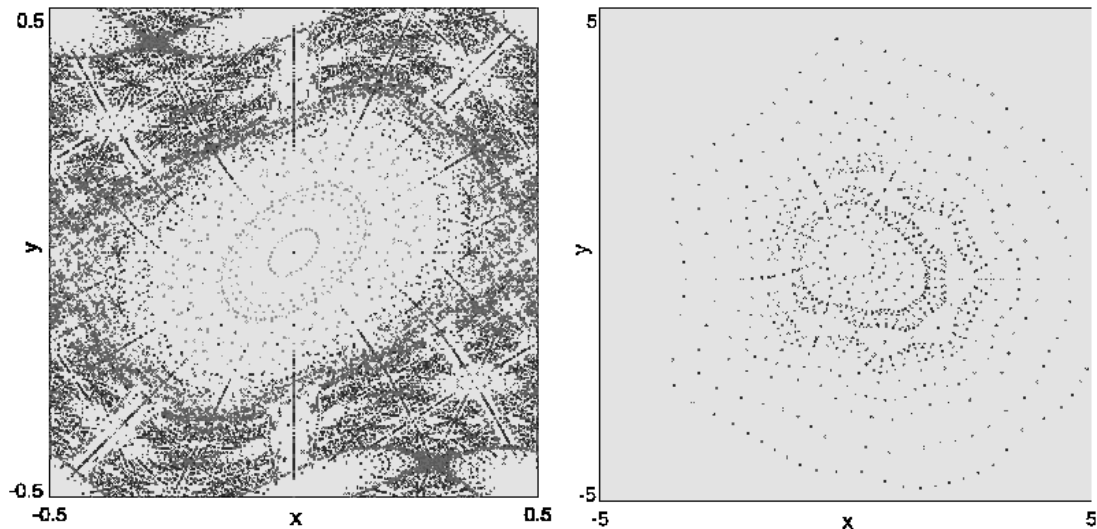


Figure 8: Periodic orbits up to period $p = 40$ for the SM (14) for $k = 0.9$ (left panel) and for the BM (15) for $\omega = 0.14$ (right panel). Different gray-scales correspond to periodic orbits with different kind of stability.

can locate a big fraction of the real periodic orbits. Actually by applying the characteristic bisection method on the cells of a lattice formed by 2000×2000 grid points we were able to compute a sufficient number of the periodic orbits with period up to 40, for the SM (figure 8, left panel) and the BM (figure 8, right panel). The computed periodic orbits give us a clear picture of the dynamics of these maps.

4 Synopsis

We have studied the applicability of various numerical methods, based on the topological degree theory, for locating high period periodic orbits of 2D area preserving maps.

In particular we have used the Kronecker integral and applied the Stenger's method for finding the TD in a bounded region of the phase space. If the TD has a non-zero value we know that there exist at least one periodic orbit in the corresponding region. The computation of the TD for an appropriate set of equations allows us to find the exact number of periodic orbits. We also applied the characteristic bisection method on a mesh in the phase space for locating the various fixed points.

The main advantage of all these methods is that they are not affected by accuracy problems in computing the exact values of the various functions used, as, the only computable information needed is the algebraic signs of these values.

We have applied the above-mentioned methods to 2D symplectic maps defined on \mathbb{R}^2 and on the torus. The methods for computing the TD are applied to continuous regions of the phase space, so their use for maps on the torus is limited to regions where no discontinuity curves exist. On the other hand the characteristic bisection method proved to be very efficient for all different types of maps, as, it allowed us to compute a big amount of the real fixed points of period up to 40 in reasonable computational times.

Acknowledgments

Ch. Skokos thanks the LOC of the conference for its financial support. Ch. Skokos was also supported by 'Karatheodory' post-doctoral fellowship No 2794 of the

University of Patras and by the Research Committee of the Academy of Athens (program No 200/532).

References

- [1] Bazzani A., Servizi G., Todesco E. and Turchetti G., 1994, CERN Yellow Report 9402.
- [2] Chiricov B. V., 1979, *Phys. Rep.*, 52, 263.
- [3] Cronin J., 1964, *Fixed points and topological degree in nonlinear analysis*, Mathematical Surveys No. 11, Amer. Math. Soc., Providence, Rhode Island.
- [4] Kalantonis V. S., Perdios E. A., Perdiou A. E. and Vrahatis M. N., 2001, *Cel. Mech. Dyn. Astr.*, 80, 81.
- [5] Kronecker L., 1895, *Werke*, Vol. 1, Leipzig, Teubner.
- [6] Lloyd N. G., 1978, *Degree Theory*, Cambridge University Press, Cambridge.
- [7] Mourrain B., Vrahatis M.N., and Yakoubsohn J.C., 2002, *J. Compl.*, 18, 612.
- [8] Perdios E. A., Kalantonis V. S. and Vrahatis M. N., 2002, *Cel. Mech. Dyn. Astr.*, 84, 231.
- [9] Picard E., 1892, *J. Math. Pure Appl.* (4e série), 8, 5.
- [10] Picard E., 1922, *Traité d'analyse*, 3rd ed., Chap. 4.7., Gauthier-Villars, Paris.
- [11] Polymilis C., Skokos Ch., Kollias G., Servizi G. and Turchetti G., 2000, *J. Phys. A*, 33, 1055.
- [12] Stenger F., 1975, *Numer. Math.*, 25, 23.
- [13] Vrahatis M. N., 1988, *ACM Trans. Math. Software*, 14, 312.
- [14] Vrahatis M. N., 1988, *ACM Trans. Math. Software*, 14, 330.
- [15] Vrahatis M. N., 1989, *Proc. Amer. Math. Soc.*, 107, 701.
- [16] Vrahatis M. N., 1995, *J. Comp. Phys.*, 119, 105.
- [17] Vrahatis M. N., Bountis T. C. and Kollmann M., 1996, *Inter. J. Bifurc. Chaos*, 6, 1425.
- [18] Vrahatis M. N., Isliker H. and Bountis T. C., 1997, *Inter. J. Bifurc. Chaos*, 7, 2707.
- [19] Vrahatis M. N., Perdiou A. E., Kalantonis V. S., Perdios E. A., Papadakis K., Prosmiiti R. and Farantos S. C., 2001, *Comp. Phys. Com.*, 138, 53.